Clinical & Experimental Immunology
The Journal of Translational Immunology

Clinical and Experimental Immunology ORIGINAL ARTICLE doi:10.1111/cei.12662

Bioenergetic analysis of human peripheral blood mononuclear cells

N. Jones, J. Piasecka, A. H. Bryant, R. H. Jones, D. O. F. Skibinski, Nigel. J. Francis and C. A. Thornton
Institute of Life Science, College of Medicine, Swansea University, Swansea, UK

Accepted for publication 28 May 2015
Correspondence: Professor C. A. Thornton, Institute of Life Science, College of Medicine, Swansea University, Swansea, UK.
E-mail c.a.thornton@swansea.ac.uk

Summary

Leucocytes respond rapidly to pathogenic and other insults, with responses ranging from cytokine production to migration and phagocytosis. These are bioenergetically expensive, and increased glycolytic flux provides adenosine triphosphate (ATP) rapidly to support these essential functions. However, much of this work is from animal studies. To understand more clearly the relative role of glycolysis and oxidative phosphorylation in human leucocytes, especially their utility in a translational research setting, we undertook a study of human peripheral blood mononuclear cells (MNCs) bioenergetics. Glycolysis was essential during lipopolysaccharide (LPS)-mediated interleukin (IL)−1β, IL-6 and tumour necrosis factor (TNF)-α production, as 2-deoxy-D-glucose decreased significantly the output of all three cytokines. After optimizing cell numbers and the concentrations of all activators and inhibitors, oxidative phosphorylation and glycolysis profiles of fresh and cryopreserved/resuscitated MNCs were determined to explore the utility of MNCs for determining the bioenergetics health profile in multiple clinical settings. While the LPS-induced cytokine response did not differ significantly between fresh and resuscitated cells from the same donors, cryopreservation/resuscitation significantly affected mainly some measures of oxidative phosphorylation, but also glycolysis. Bioenergetics analysis of human MNCs provides a quick, effective means to measure the bioenergetics health index of many individuals, but cryopreserved cells are not suitable for such an analysis. The translational utility of this approach was tested by comparing MNCs of pregnant and non-pregnant women to reveal increased bioenergetics health index with pregnancy but significantly reduced basal glycolysis and glycolytic capacity. More detailed analysis of discrete leucocyte populations would be required to understand the relative roles of glycolysis and oxidative phosphorylation during inflammation and other immune responses.

Keywords: cell activation, cytokines, human, inflammation

Introduction

Cell viability and effector functions are dependent upon energy production in the form of adenosine triphosphate (ATP) [1]. Typically, glucose is taken up by a cell to generate pyruvate via glycolysis; pyruvate is oxidized into acetyl co-enzyme A (CoA), which enters the tricarboxylic acid (TCA) or Krebs cycle [1]; the Krebs cycle yields nicotinamide adenine dinucleotide (NADH) for downstream energy production via oxidative phosphorylation within the mitochondria [2]. Glycolysis yields a net of two ATP molecules per molecule of glucose, whereas oxidative phosphorylation yields in excess of 30 molecules of ATP per molecule of glucose [3]. Other fuels, such as fatty acids, may be utilized for ATP generation. They are fed typically into the TCA cycle within the mitochondria via the enzyme carnitine palmitoyltransferase 1 (CPT1) [4]. Under aerobic conditions most of a healthy cell's energy is derived via oxidative phosphorylation; however, cancer cells are reprogrammed metabolically for increased glycolysis, the so-called Warburg effect [5]. While inefficient, increased glycolytic flux generates ATP molecules

rapidly, with glucose used 12 times faster in glycolysis *versus* oxidative phosphorylation [5,6] providing the energy needed for the production of biomolecules and other effector functions [7].

Leucocytes are also reported to undergo the Warburg effect upon activation via pathogenic and other stimuli [8–10]. Regarding cancer cells, increased glycolysis allows the rapid production of molecules, such as cytokines, chemokines and anti-microbial peptides, and supports processes such as migration and phagocytosis [5,11,12]. This phenomenon is also seen under hypoxic conditions, whereby glucose is converted to lactic acid [11], and might explain why monocytes and macrophages exhibit extended hypoxic survival [2]. Work, mainly from mouse models, has shown that for B and T lymphocytes and natural killer (NK) cells increased glycolytic flux enables clonal expansion [13–16], accompanied by the production of proinflammatory cytokines such as interferon (IFN)-γ [14,16,17]. Glucose-dependent activation of human monocytes by lipopolysaccharide (LPS) results in a switch to heavily glycolytic metabolism supporting the production of cytokines [18]. This metabolic reprogramming of leucocytes is accompanied by elevated production of lactate due to the rapid generation of ATP [9,18], and lactate itself has been reported to have anti-microbial properties [10] and a role in interleukin (IL)-17A production [19].

The Bioenergetics Health Index (BHI) has been suggested as a rapidly calculated single value that reflects mitochondrial health [20]. The BHI takes into account beneficial parameters such as maximum respiration and ATP-linked respiration while incorporating deleterious parameters such as proton leak and reduced mitochondrial reserve capacity. Consequently, the BHI might offer a rapid means of detecting mitochondrial dysfunction allowing early disease diagnosis and facilitating precision medicine approaches to disease management [20]. Monitoring the BHI in various clinical settings, including cohort studies, translational medicine, immunotherapeutics and even screening of drug toxicity, might be achieved using peripheral blood mononuclear cells as a readily accessible source of patient material. The emerging field of mitochondrial medicine has been demonstrated with techniques such as the J-aggregate-forming lipophilic cation 5,5′,6,6′-tetraethyl-benzimidazolocarbocyanine iodide (JC-1) assay that detects the loss of mononuclear cell (MNC) mitochondrial membrane potential, leading to MNC apoptosis among HIV-positive patients [21]. The diagnostic use of MNC respiratory parameters as potential disease biomarkers has been correlated positively with a loss of mitochondrial respiratory chain enzymes and function with lipoatrophy [22]. It has also been suggested that bioenergetic disruption of monocytes and macrophages leads to metabolic conditions such as chronic kidney disease and atherosclerosis [23,24]. Non-invasive extracellular bioflux analysis of cells allows quantification of the ATP-producing respiratory processes via measurement of oxygen consumption rate (OCR) for oxidative phosphorylation (OP) and extracellular acidification (ECAR) for glycolysis. In this work, we have studied human peripheral blood MNCs to not only understand more clearly the bioenergetics profile of these cells but as a potential substrate for monitoring the BHI. The impact of cryopreservation was considered, as bulk analysis of cells from different donors can be of benefit in settings such as cohort studies; this has been shown recently to have a negative impact on the BHI [25]. To test the utility of using MNC BHI in a clinical setting we compared MNCs from pregnant and non-pregnant women. While little is known currently about the metabolism of haematopoietic cells from pregnant women, changes related to insulin sensitivity and the handling of glucose by skeletal muscle and adipose tissue are well documented as a normal physiological response from the second trimester [26,27].

Materials and methods

Samples

Human peripheral blood was collected between 08:30 and 10:00 h from healthy, non-fasted individuals into heparinized Vacuettes™ (Greiner Bio-one, Frickenhausen, Germany) and processed within 10 min of collection. Peripheral blood was also collected from healthy pregnant women at >37 weeks' gestation and matched with samples from non-pregnant women aged 20–40 years. All samples were collected with informed written consent, and ethical approval was obtained from Wales Research Ethics Committee 6 (13/WA/0190; 11/WA/0040).

Mononuclear cell isolation

Mononuclear cells were isolated by layering whole blood (1 : 1) onto Histopaque (Sigma-Aldrich, Poole, UK) prior to centrifugation at 805 ***g*** for 20 min at room temperature. MNCs were removed and washed twice with RPMI-1640 (Life Technologies, Paisley, UK) by centrifugation at 515 ***g***. The MNC pellet was resuspended in media specific for the downstream assay and cell density determined using the Countess® automated cell counter (Life Technologies). For the pregnancy section of the study, red blood cells were removed selectively from both non-pregnant and pregnant blood samples using glycophorin A (CD235a) microbeads (autoMACS; Miltenyi Biotec, Cologne, Germany), as described by the manufacturer.

Cryopreservation and resuscitation

MNCs were cryopreserved and resuscitated using the (CTL)-Cyro™ ABC media kit (Cellular Technology Limited, Birmingham, UK), as per the manufacturer's instructions. Briefly, cells were cryopreserved by resuspending in

CTL-CryoC media and the slow addition of an equal volume of solution CryoAB. Cells were then transferred to a cryovial and stored at −80°C. Cells were resuscitated by thawing in a 37°C water bath and the slow addition of 5 ml of CTL-thaw solution. Resuscitated cells were left for 30 min in RPMI-1640 5% fetal calf serum (FCS; HyClone, ThermoFisher Scientific, Waltham, MA, USA) and 0·2% 2-mercaptoethanol (Life Technologies) to reacclimatize. Flow cytometry was used to monitor the cellular content of fresh and resuscitated MNCs.

Effect of glycolysis and respiratory inhibitors on cytokine production

MNCs were cultured at 5×10^5 cells/500 μl of RPMI/5% FCS/0·5 μM 2-mercaptoethanol (ME) ± lipopolysaccharide (LPS) (Ultrapure, 10 ng/ml; InvivoGen, San Diego, CA, USA) at 37°C in 5% CO_2-in-air for 24 h. Additional treatments included for the 24 h incubation were: 2-deoxy-D-glucose (2-DG; 0, 0·5, 1 and 2·5 mM; Sigma, Poole, UK); rotenone (1, 2 μM; Seahorse Bioscience, Copenhagen, Denmark) and/or pyruvate (1 mM; Life Technologies). After 24 h, cultures were centrifuged at 515 ***g*** for 7 min and cell-free supernatants removed and stored at −20°C until analysis of lactate dehydrogenase (LDH) and cytokines by enzyme-linked immunosorbent assays (ELISAs).

Lactate dehydrogenase cytotoxicity assay

Cytotoxicity was measured using a lactate dehydrogenase cytotoxicity assay, as per the manufacturer's instructions (LDH-Cytotoxicity Assay Kit II; Abcam, Cambridge, UK). Briefly, 10 μl culture supernatant was mixed with 100 μl LDH reaction mix containing a WST substrate (tetrazolium salt substrate with the chemical formula of 4-[3-(4-iodophenyl)-2-(4-nitrophenyl)−2H-5-tetrazolio]-1,3-benzene disulphonate sodium salt) and incubated at room temperature for 30 min and absorbance at 450 nm measured. A positive control of lysed cells was used: 5×10^5 cells/100 μl with 10 μl cell lysis solution (provided in the kit) at 37°C for 24 h.

ELISA

Analysis of cytokines using ELISA was as per the manufacturer's instructions – IFN-γ (Ready-Set-Go; eBioscience, San Diego, CA, USA), IL-1β, IL-6 and tumour necrosis factor (TNF)-α (DuoSets; R&D Systems, Abingdon, UK).

Bioenergetics analysis

Adhesion to the bioflux plate. As the majority of MNCs (the exception being monocytes) are non-adherent, Cell-Tak (Corning, MA, USA) was used at 3·5 μg/cm^2 per well according to the manufacturer's instructions to attach them to the XF^{e}24 bioflux plate (Seahorse Bioscience) used for bioenergetics analysis. The potential for Cell-Tak to activate MNCs was determined. MNCs were seeded at $2{\cdot}5 \times 10^5$ cells per well with or without Cell-Tak and stimulated ± 10 ng/ml LPS (as before) as a prototypic stimuli of monocytes in particular with IL-6 measured as the output; and CytoStim (1/200 from stock; Miltenyi Biotec) or phytohaemagglutinin (PHA, 1 μg/ml; Sigma) for 48 h at 37°C as T cell stimuli in particular with IFN-γ measured as the output.

Oxidative phosphorylation. Mitochondrial stress is measured via the initial addition of oligomycin to block ATP synthase. Then, carbonyl cyanide-*p*-trifluoromethoxyphenylhydrazone (FCCP), a proton ionophore that selectively removes the regulation of the proton gradient [28], is injected allowing the maximum respiration rate to be determined. Finally, rotenone and anti-mycin A inhibit complex I and III, respectively, of the electron transport chain.

Cells were resuspended in XF Assay media (Seahorse Bioscience) supplemented with 5·5 mM glucose and 1 mM pyruvate as pre-optimized for use with the Mito-Stress kit (Seahorse Bioscience). Cells were seeded onto a XF^{e}24 bioflux plate (Seahorse Bioscience) at a pre-optimized final concentration of $2{\cdot}5 \times 10^5$ cells/80 μl/well and centrifuged gently with no brake at 40 ***g***, and the plate then rotated 180° before centrifugation again at 80 ***g*** to encourage adhesion to the plate and the forming of an evenly dispersed monolayer. Cells were then incubated at 37°C for 30 min before 445 μl prewarmed XF Assay media was added to each well. Cells were returned to the incubator at 37°C for a further 15 min and then processed using the XF^{e}24 Extracellular Flux Analyzer (Seahorse Bioscience). Mitochondrial function was measured as OCR after injections of 0·5 μM oligomycin (ATP synthase inhibitor), 1 μM FCCP (electron transport chain accelerator) and 1 μM anti-mycin A (complex III inhibitor) plus 1 μM rotenone (complex I inhibitor), according to the manufacturer's instructions.

Glycolysis. Glycolysis is measured via the initial injection of glucose, the carbohydrate precursor of glycolysis. Oligomycin is then added to inhibit ATP synthase as above, and finally 2-DG is injected as a competitive inhibitor of glycolysis, blocking the enzyme activity of hexokinase and thus halting glycolysis.

Cells were resuspended in XF assay media for use with the glycolysis stress kit (Seahorse Bioscience). Cells were attached to the bioflux plates as described above and glycolysis was then measured as ECAR after injections of differing glucose concentrations (0, 2, 5·5, 11·1 and 25 mM), 0·75 μM oligomycin (inhibits ATP synthase forcing the cell to utilize glycolysis only) and the competitive inhibitor 2-DG (100 mM).

Total protein estimation. After completion of the bioenergetics assays, the media was removed and the cells washed once with PBS (Life Technologies). Lysis buffer (50 μl; BD

Biosciences, Franklin Lakes, NJ, USA) was then added to each well and the plate stored at −20°C for a minimum of 24 h. A bicinchoninic acid (BCA; Sigma) assay on thawed lysates was compared to a bovine serum albumin (BSA) protein standard (Sigma). Briefly, 10 μl of lysate was mixed with a 50 : 1 ratio of BCA solution to copper II sulphate pentahydrate 4% solution, respectively (Sigma) and incubated at 37°C for 30 min. The absorbance was then measured at 562 nm.

Data analysis

OCR and ECAR values were normalized to protein concentrations of the respective wells with the use of Microsoft Excel version 14·4·4 (Microsoft, Irving, TX, USA).

The various respiratory parameters were calculated using the following methods using data obtained from the Seahorse XF^e analyser.

Mitochondrial stress assay. Non-mitochondrial respiration is the difference between the average of the final three measurements after injection of anti-mycin A/rotenone; proton leak is measured as the difference between the average of the final three measurements and the averaged three data points after oligomycin injection. Removing the non-mitochondrial respiration value from the initially averaged three measurements identifies basal respiration. ATP-linked respiration was calculated by removing the proton leak from the basal respiration value, whereas maximal respiration was measured by taking the non-mitochondrial respiration from the averaged three data points after FCCP injection. Finally, the reserve respiratory capacity was measured by maximal respiration – basal respiration (Table 1) [28].

Glycolysis stress assay. An average of the first and last three measurements gives a measure of non-glycolytic acidification. After glucose injection the averaged three corresponding points were used to calculate basal glycolysis after removing the non-glycolytic acidification. Taking the averaged three measurements after oligomycin injection and removing the non-glycolytic acidification yields glycolytic capacity. Finally, the glycolytic reserve was calculated by glycolytic capacity – basal glycolysis (Table 1).

Flow cytometry

To monitor T cell subset and monocyte content of fresh and resuscitated MNCs 2.5×10^5 cells were incubated with anti-CD3 eFluor®450 (mIgG2a, clone OKT3; eBioscience), anti-CD4 AlexaFluor®647 (mIgG2b, clone OKT4; eBioscience), anti-CD8 phycoerythin (PE) (mIgG1, clone HIT8a; eBioscience) and anti-CD14 eFluor®450 (mIgG1, clone 61D3; eBioscience) antibodies using standard techniques. MNC subpopulation monitoring of pregnant and non-pregnant samples was performed as above, with the inclusion of anti-CD19 FITC (mIgG1, clone HIB19; BioLegend, San Diego, CA, USA). Cells were acquired (FACSAria I; BD Biosciences) and downstream analysis was performed with Kaluza version 1·3 (Beckman Coulter, Fullerton, CA, USA).

Statistics

Statistical analysis was performed using SPSS version 20 (IBM, Armonk, NY, USA). Data are represented as the mean ± standard error of the mean. The one-sample Kolmogorov–Smirnoff test was used to test for normality. Any substantial deviation from normality resulted in a non-parametric test being used, otherwise it was considered appropriate to use parametric statistics. One-way analysis of variance (ANOVA) was used to compare the Cell-Tak activation, and 2-deoxy-D-glucose cytokine output with Bonferroni *post-hoc* tests. Tukey's *post-hoc* test was performed on the metabolic cytokine output data. Paired-samples *t*-test was used for fresh *versus* resuscitated oxidative phosphorylation data, fresh *versus* resuscitated MNC cytokine outputs, pregnant *versus* non-pregnant oxidative phosphorylation and glycolysis data and flow cytometry cell population number data, including pregnant *versus* non-pregnant populations. A three-way ANOVA was used for the fresh *versus* resuscitated glycolysis data.

Table 1. Various respiratory parameters calculated using the bioenergetic profiles produced by the Seahorse XF analyser.

Parameter	Calculation*
Proton leak	Difference between last three and oligomycin injection measurements
Non-mitochondrial respiration	Measurement after anti-mycin A/rotenone
Basal respiration	Initial three measurements – non-mitochondrial respiration
ATP-linked respiration	Basal respiration – proton leak
Maximal respiration	Difference between FCCP and anti-mycin A/rotenone injections
Reserve respiratory capacity	Basal respiration – maximal respiration
Glycolysis	Glucose injection – non-glycolytic acidification
Glycolytic capacity	Oligomycin injection – non-glycolytic acidification
Glycolytic reserve	Glycolytic capacity – glycolysis
Non-glycolytic acidification	Averaged first and last triplicate measurements

*All triplicate measurements are averaged. ATP = adenosine triphosphate; FCCP = carbonyl cyanide-4-(trifluoromethoxy)phenylhydrazone.

All experiments have replicate sample sizes of at least three and significant values were taken as $P < 0{\cdot}05$ graphically denoted as $^{*}P \leq 0{\cdot}05$, $^{**}P \leq 0{\cdot}01$ and $^{***}P \leq 0{\cdot}001$.

Results

2-DG down-regulates LPS-mediated cytokine production

Before detailed investigation of glycolysis and oxidative phosphorylation by MNCs, the role of glycolysis in a response by MNCs was determined. LPS treatment of MNCs stimulated production of cytokines IL-1β, IL-6 and TNF-α, as expected. The competitive glycolysis inhibitor 2-DG (0, 0·5, 1 and 2·5 mM) reduced LPS-mediated cytokine production significantly for all three cytokines (Fig. 1a).

To explore this further, the cytokine output in the presence of a number of treatments, 2-DG, 2-DG + pyruvate (1 mM and 2 mM), pyruvate (1 and 2 mM), rotenone (1 and 2 μM) was measured. The ability of pyruvate to bypass the glycolytic step inhibited by 2-DG was considered but had a negligible effect on the inhibitory effect of 2-DG (Fig. 1b). Similarly, rotenone (a complex I inhibitor), which inhibits the electron transport chain, had no significant effect on cytokine output. Although TNF-α levels appeared more susceptible to the effects of rotenone, this was not significant (Fig. 1b). There was no measureable cell death detected via the LDH assay (data not shown).

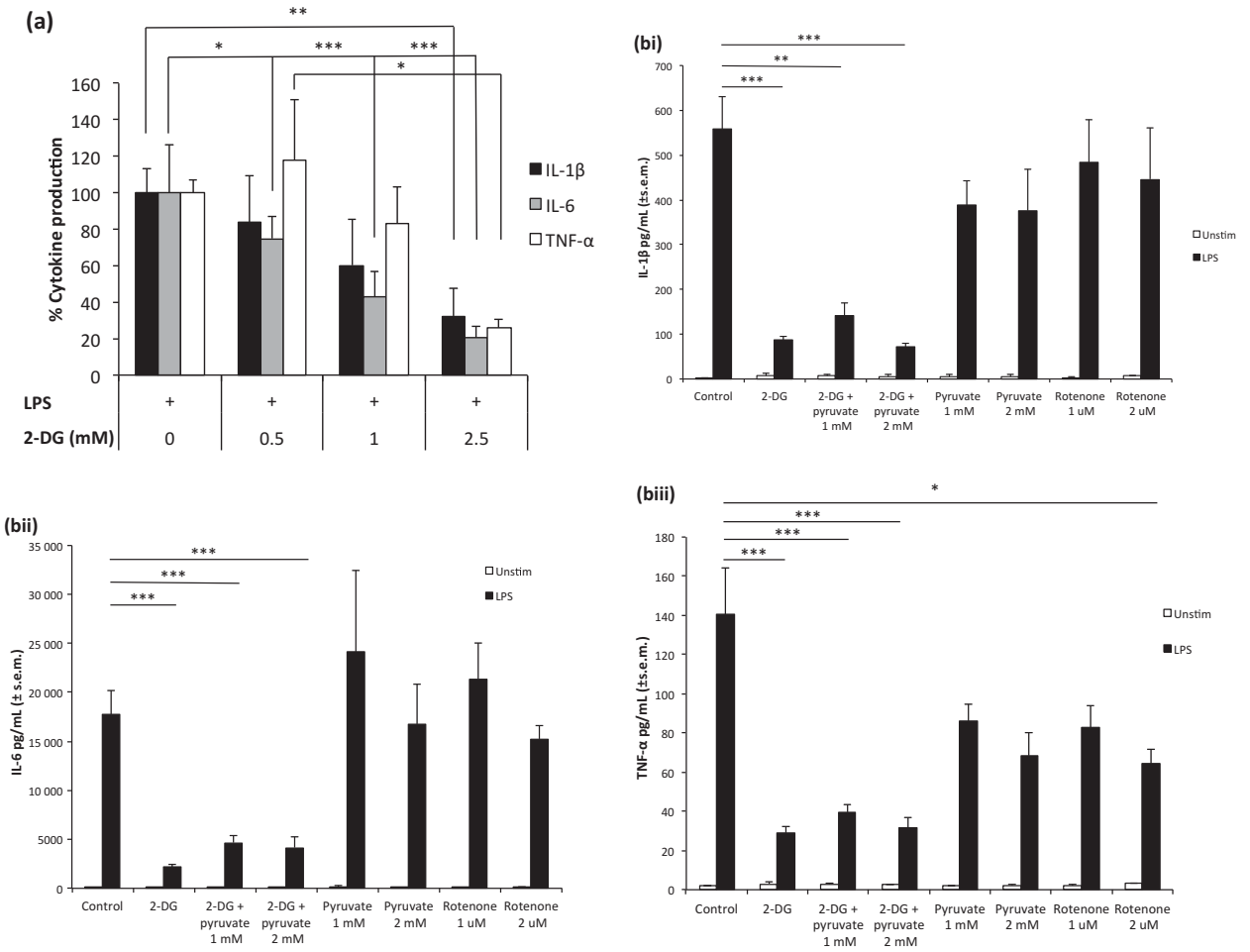

Fig. 1. The effect of inhibitors of glycolysis and oxidative phosphorylation on lipopolysaccharide (LPS)-mediated cytokine outputs of human peripheral blood mononuclear cells (MNCs). (a) Interleukin (IL)−1β, IL-6 and tumour necrosis factor (TNF)-α after stimulation ± LPS (10 ng/ml) for 24 h in the presence of varying concentrations of 2-deoxy-D-glucose (2-DG, 0–2·5 mM). Data represented as percentage of the LPS control. Statistical significance compared to LPS was evaluated using one-way analysis of variance (ANOVA) with Bonferroni's *post-hoc* test ($n = 5$; $^{*}P \leq 0{\cdot}05$, $^{**}P \leq 0{\cdot}01$, $^{***}P \leq 0{\cdot}001$). Significance also observed (not shown on graph) regarding cytokine IL-6 production treated with 0·5 mM 2-DG/LPS compared to both 1 and 2·5 mM 2-DG/LPS. (bi,ii,iii) Three cytokines measured under the same experimental conditions. Cytokine output (IL-1β, IL-6 and TNF-α) after stimulation ± LPS for 24 h in the presence of various respiratory inhibitors or substrates (pyruvate; 1 + 2 mM, 2-DG; 2·5 mM and rotenone; 1 + 2 μM). Data are shown as pg/ml ± standard error of the mean. Statistical significance compared to LPS was evaluated using one-way ANOVA with Tukey's *post-hoc* test ($n = 4$; $^{*}P \leq 0{\cdot}05$, $^{**}P \leq 0{\cdot}01$, $^{***}P \leq 0{\cdot}001$).

The effect of Cell-Tak on MNC cytokine outputs

Bioenergetic analysis using extracellular flux analysis requires an adherent cell monolayer, so for some cell types such as lymphocytes, which are typically not adherent, a cell adhesive such as Cell-Tak is required. Therefore, the potential of Cell-Tak to activate MNCs was considered. Cell-Tak and/or gentle centrifugation had no effect on IL-6 or IFN-γ levels from otherwise unstimulated cells (Fig. 2a,b). However, while there was no difference in cytostimulated or PHA-stimulated IFN-γ levels from MNCs, irrespective of the presence of Cell-Tak or gentle centrifugation (Fig. 2a), the adherence of MNCs to Cell-Tak was associated with a significant increase in LPS-stimulated IL-6 ($P = 0{\cdot}006$ *versus* no Cell-Tak + gentle centrifugation, $P = 0{\cdot}003$ *versus* no Cell-Tak/no centrifugation; Fig. 2b) but background levels in the unstimulated controls remained unaffected.

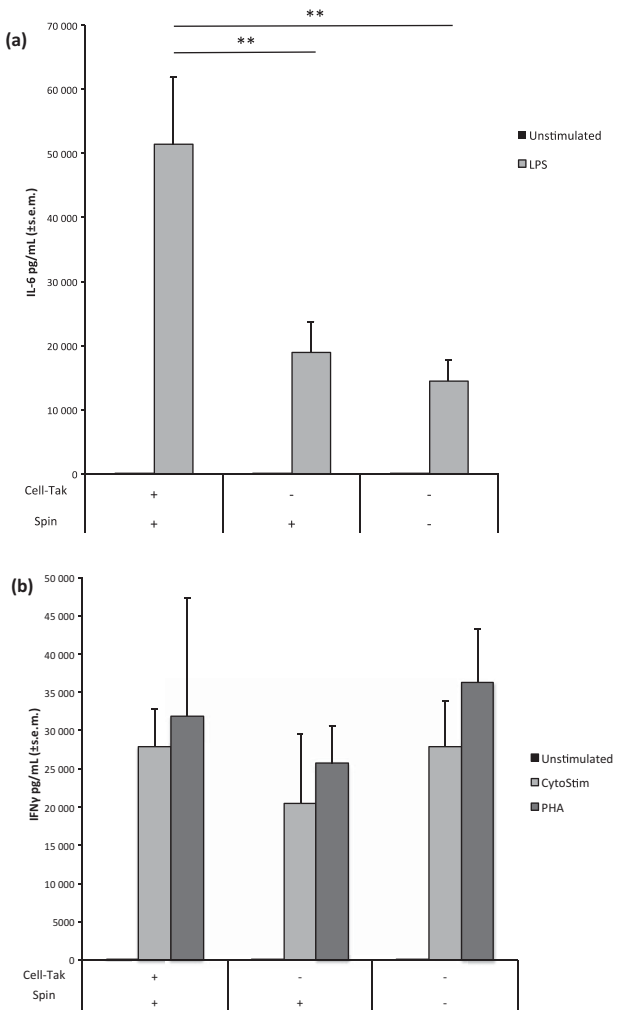

Fig. 2. The effect of Cell-Tak and gentle centrifugation on cytokine production by mononuclear cells (MNCs). (a) Lipopolysaccharide (LPS)-stimulated interleukin (IL)-6 levels (pg/ml ± standard error of the mean, $n = 3$) after 24 h incubation, and (b) cytostimulated and phytohaemagglutinin (PHA)-stimulated interferon (IFN)-γ levels (pg/ml ± standard error of the mean, $n = 3$) after 48 h incubation from cells ± Cell-Tak with or without gentle centrifugation (spin). Statistical significance was measured using a one-way analysis of variance (ANOVA), $^{**}P \leq 0{\cdot}01$.

Bioenergetic profile of mononuclear cells

To confirm that MNCs gave the expected profile of OCR linked to oxidative phosphorylation and ECAR to proton expulsion related to glycolysis, a preliminary experiment was carried out by first uncoupling the electron transport chain with 2,4-DNP (100 μM), then inhibiting glycolysis with 2-DG (100 mM) and finally inhibiting complex I via rotenone (2 μM). This resulted in an observable and expected change in OCR/ECAR (Fig. 3a) [29].

Oxidative phosphorylation and glycolysis were then studied in fresh MNCs and matched cryopreserved/resuscitated MNCs (Table 2). This was performed to explore the utility of batch analysis of cryopreserved MNCs as part of cohort studies and in other translational medicine settings. The cellular content (monocytes and T cell subsets) did not differ significantly between the matched fresh and resuscitated cells (Table 3), nor did LPS-stimulated IL-1β, IL-6 and TNF-α (Fig. 4). There was no difference in cell death between fresh and resuscitated cells cultured with/without LPS for 24 h as measured using the LDH assay (data not shown).

For bioenergetics analysis an optimized MNC density of $2{\cdot}5 \times 10^5$ cells/well was used. The mitochondrial stress assay injections were also pre-optimized: oligomycin (0·5 μM), FCCP (1 μM), anti-mycin A and rotenone (both 1 μM). The mitochondrial stress assay gave a typical profile in both fresh and resuscitated cells (Fig. 3b), but there were significant differences in basal respiration ($P = 0{\cdot}021$), ATP-linked respiration ($P = 0{\cdot}043$ and non-mitochondrial respiration ($P = 0{\cdot}011$) for fresh *versus* resuscitated; maximum respiration was near significant ($P = 0{\cdot}057$), but there was no difference in reserve respiratory capacity and proton leak. The significant reduction of ATP-linked respiration and increase in non-mitochondrial respiration has detrimental affects on the BHI of resuscitated cells ($2{\cdot}90 \pm 0{\cdot}71$) in comparison to fresh ($18{\cdot}28 \pm 5{\cdot}71$).

The glycolysis stress assay was carried out with varying concentrations of glucose (0, 2, 5·5, 11·1 and 25 mM; Fig. 3c,d). As expected, MNCs deprived of glucose (0 mM) had lower glycolytic parameters, with the exception of glycolysis-independent non-glycolytic acidification. Provision of increasing concentrations of the substrate glucose (2, 5·5, 11·1 and 25 mM) produced an increase in glycolysis and the glycolytic capacity/reserve for both fresh and resuscitated cells. There was a statistically significant difference between fresh and resuscitated cells at different glucose doses (0, 2, 5·5, 11·1 and 25 mM) for glycolytic reserve ($P < 0{\cdot}001$ for both dose and conditions), glycolytic

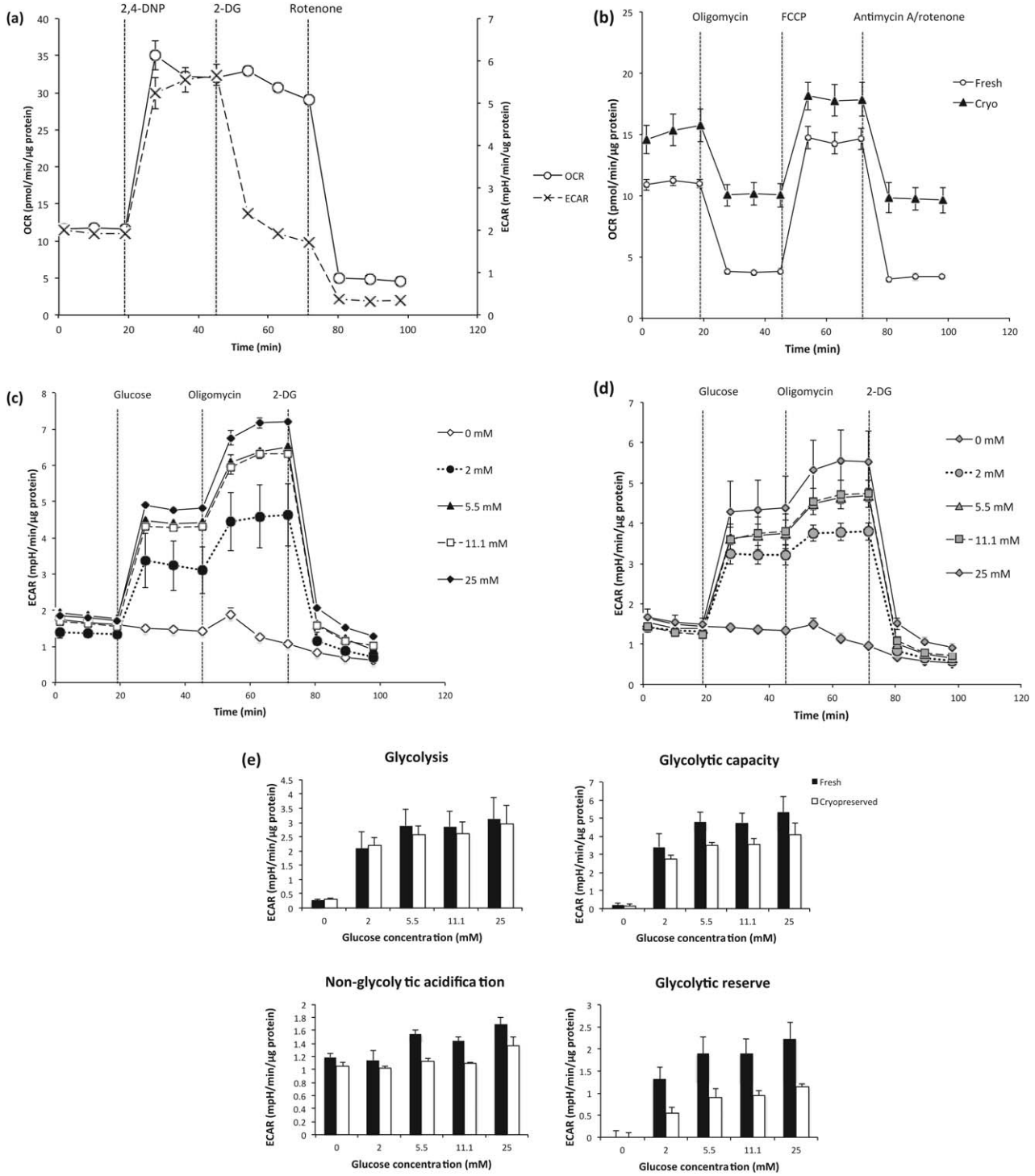

Fig. 3. The bioenergetics profile of mononuclear cells (MNCs). (a) Combinatory metabolic profile of fresh MNCs with injections 2,4-dinitrophenol (2,4-DNP, 100 μM), 2-DG (100 mM) and rotenone (2 μM), showing both oxygen consumption rate (OCR) and extracellular acidification rate (ECAR) values ($n = 4$). (b) Mitochondrial stress profile of matched fresh and cryopreserved/resuscitated MNCs with injections oligomycin (0·75 μM), carbonyl cyanide-4-(trifluoromethoxy)phenylhydrazone (FCCP; 1 μM) and anti-mycin A/rotenone (both 1 μM). (c) Fresh and (d) cryopreserved mononuclear cell glycolytic stress profile with differing concentrations of glucose (0, 2, 5·5, 11·1 and 25 mM), along with oligomycin (0·75 μM) and 2-DG (100 mM). (e) Comparative glycolytic parameters of matched fresh *versus* cryopreserved/resuscitated MNCs. All data are normalized to μg protein and shown as mean ± standard error of the mean ($n = 4$). Statistical differences are reported in the text.

Table 2. Comparative oxidative phosphorylation parameters of matched fresh *versus* cryopreserved/resuscitated mononuclear cells (MNCs).

Respiratory parameter	Fresh OCR (± s.e.m.; pmoles/min/μg protein)	Cryopreserved OCR (± s.e.m.; pmoles/min/μg protein)	*P*-value
Basal respiration	7·71 (± 0·35)	5·50 (± 0·31)	0·021
ATP-linked respiration	7·23 (± 0·31)	5·15 (± 0·38)	0·043
Non-mitochondrial respiration	3·31 (± 0·18)	9·73 (± 1·06)	0·011
Maximal respiration	11·23 (± 0·76)	8·19 (± 0·29)	0·057
Reserve respiratory capacity	3·52 (± 0·66)	2·69 (± 0·23)	0·306
Proton leak	0·47 (± 0·08)	0·35 (± 0·14)	0·437
BHI	18·28 (± 5·71)	2·90 (± 0·71)	0·785

ATP = adenosine triphosphate; BHI = Bioenergetics Health Index; OCR = oxygen consumption rate; s.e.m. = standard error of the mean.

Table 3. Percentage of $CD14^+$ monocytes, $CD3^+$ T cells and the main T cell subsets ($CD3^+/CD4^+$ and $CD3^+/CD8^+$) as a percentage of total $CD3^+$ T cells in freshly isolated and resuscitated mononuclear cell (MNC) preparations. The CD4 : CD8 ratio is also shown ($n = 7$).

Cell population	Fresh ± s.e.m. (%)	Resuscitated ± s.e.m. (%)	*P*-value
$CD14^+$	12·59 (± 1·52)	16·66 (± 1·69)	0·083
$CD3^+$	64·92 (± 2·05)	71·02 (± 2·35)	0·100
$CD3^+CD4^+$	64·78 (± 2·84)	63·71 (± 2·97)	0·821
$CD3^+CD8^+$	24·07 (± 2·06)	24·39 (± 2·62)	0·939
$CD4^+$: $CD8^+$ ratio	2·69 (± 0·34)	2·61 (± 0·47)	0·950

s.e.m. = standard error of the mean.

capacity ($P < 0·001$ dose and $P = 0·007$ for conditions) and non-glycolytic acidification ($P < 0·001$ for both). There was a significant difference only for glucose dose ($P < 0·001$).

Glycolysis and glycolytic capacity levels of MNCs from pregnant *versus* non-pregnant women

To ensure that differences in cellular composition of MNCs did not differ between the two groups and impact on bioenergetics parameters, flow cytometry was used to monitor major subsets. There was no significant difference in any of the major cell populations – monocytes, $CD4^+$ T cells, $CD8^+$ T cells and B cells – of pregnant *versus* non-pregnant women (Table 4). Mitochondrial function was assessed using the same mitochondrial stress injections as above (Fig. 5a). There was no significant difference for any of the mitochondrial stress respiratory parameters between non-pregnant and pregnant MNCs (Table 5). The BHI of pregnant MNCs was elevated (30·22 ± 5·76 *versus* 15·66 ± 7·67), but this was not significant.

The glycolytic stress assay also was applied to the non-pregnant/pregnant cohort using a single, physiological concentration of glucose (5·5 mM; Fig. 5b). MNCs from pregnant women had lower basal glycolysis levels ($P = 0·0219$) and glycolytic capacity ($P = 0·0390$; Fig. 5c) compared to those from non-pregnant women. There was a significant difference between the OCR/ECAR ratio of MNCs from pregnant and non-pregnant women ($P = 0·0207$; Fig. 5d), suggesting that MNCs from pregnant women rely more heavily on OP to obtain their energy, whereas those from non-pregnant women utilize glucose metabolism, i.e. glycolysis, more.

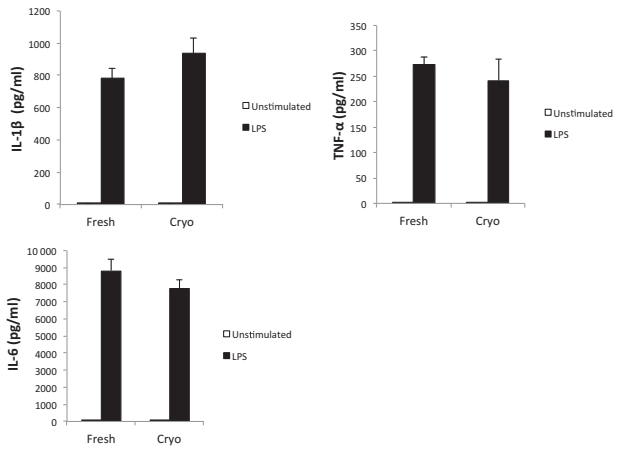

Fig. 4. Cytokine response by matched fresh *versus* cryopreserved/resuscitated mononuclear cells (MNCs). Comparative concentrations of interleukin (IL)−1β, IL-6 and tumour necrosis factor (TNF)-α from fresh and cryopreserved MNCs after treatment ± lipopolysaccharide (LPS) (10 ng/ml) for 24 h. Data are shown as pg/ml ± standard error of the mean ($n = 7$).

Discussion

Microbial products such as LPS stimulate MNCs to generate proinflammatory cytokines rapidly. Here, we show for the first time, to our knowledge, the absolute requirement for glycolysis for production of IL-1β, IL-6 and TNF-α by human mononuclear cells. By inhibiting with 2-DG the activity of hexokinase that phosphorylates glucose to glucose-6-phosphate to kick-start glycolysis, the LPS-mediated production of these cytokines was inhibited

Table 4. Percentage of $CD14^+$ monocytes, $CD19^+$ B cells, $CD3^+$ T cells, and the main T cell subsets ($CD3^+/CD4^+$ and $CD3^+/CD8^+$) as a percentage of total $CD3^+$ T cells in mononuclear cells (MNCs) from non-pregnant and pregnant women. The CD4 : CD8 ratio is also shown ($n = 7$/group).

Cell population	Non-pregnant ± s.e.m. (%)	Pregnant ± s.e.m. (%)	*P*-value
$CD14^+$	12·18 (± 2·65)	11·49 (± 2·19)	0·8114
$CD19^+$	5·26 (± 0·80)	4·97 (± 0·69)	0·7425
$CD3^+$	69·39 (± 3·61)	71·76 (± 3·21)	0·5613
$CD3^+CD4^+$	54·55 (± 1·55)	51·9 (± 2·68)	0·3054
$CD3^+CD8^+$	25·34 (± 2·08)	26·2 (± 1·69)	0·7029
$CD4^+$: $CD8^+$ ratio	1·59 (± 0·24)	2·04 (± 0·22)	0·1161

s.e.m. = standard error of the mean.

significantly in a dose-dependent manner in the absence of measurable cell death. In contrast, the complex I respiratory inhibitor rotenone did not reduce LPS-stimulated cytokine outputs significantly, suggesting that the electron transport chain, albeit a significant energy producing pathway, does not contribute directly to the formation of cytokines. These data support the hypothesis that the effector function, e.g. cytokine production, of many leucocytes is dependent upon increased glycolysis, as it provides a rapid source of ATP to enable a timely immune response [8–10], but is the first to show this for human blood mononuclear cells.

Having established a critical role for glycolysis in an effector function of MNCs, more detailed analysis was undertaken of the bioenergetics pathways operational within these cells. Extracellular flux analysis is a relatively new technique for studying the energy-producing pathways utilized by cells. As MNCs are mainly non-adherent, Cell-Tak was used to generate the adherent cell monolayer required for this method. Therefore, the potential activating effect of Cell-Tak was considered and it was found that cells adhered to Cell-Tak had significantly increased LPS-stimulated IL-6 levels. This is not due to LPS contamination of the Cell-Tak, as Cell-Tak alone did not induce IL-6 production by the MNCs, so the reasons for this remain unknown and are the subject of ongoing investigation.

MNCs used both glycolysis and oxidative phosphorylation pathways. Different glucose concentrations were used to provide a more detailed analysis of glycolysis. MNCs were deprived of glucose (0 mM), 2 mM was used as a minimal addition, 5·5 mM as a widely accepted average concentration of circulating glucose under physiological conditions [30], 11·1 mM as the general cell culture media glucose concentration, and finally 25 mM was used to provide the MNCs with excess glucose [31]; increasing glucose concentrations increased the glycolytic capacity of MNCs.

One part of this study was to consider the possibility that cryopreserved MNCs could be used to study patient cohorts in a number of clinical and translational settings. There were no differences in the cellular content of fresh *versus* cryopreserved/resuscitated cells nor the functional activity of these cells as monitored by their ability to respond to LPS for cytokine production, as reported elsewhere [32,33]. However, bioenergetics profiles were impacted by cryopreservation and resuscitation, especially mitochondrial function. Cryopreserved/resuscitated MNCs had a threefold increase in non-mitochondrial respiration probably attributable to reactive oxygen species (ROS) generation and decreased mitochondrial health of the cryopreserved cells [20]. Basal respiration and ATP-linked respiration were decreased significantly between fresh and cryopreserved/resuscitated cells, again providing evidence for damaged mitochondria [25,34,35]. Glycolysis occurs within the cytoplasm and is independent of mitochondrial health. There was no significant difference in glycolysis between fresh and cryopreserved/resuscitated MNCs, hence glycolysis-dependent LPS-stimulated IL-1β, IL-6 and TNF-α production remain unaffected. However, there was a significant difference between the glycolytic capacity, glycolytic reserve and non-glycolytic acidification, all indicating reduced bioenergetic health. Thus, the cryopreservation and resuscitation of MNCs has a detrimental effect on the bioenergetic health of the cells due to the damaging effect on the mitochondria, the main energy source of the cells. The detrimental impact of cryopreservation on MNC BHI has also been demonstrated recently by another group [25]. While a recovery period after resuscitation might prove beneficial, the impact on the cellular profile then used for bioenergetics analysis (e.g. monocytes lost due to adherence to cell culture plastics during recovery phase) led us to decide not to pursue this approach.

To test the translational utility of MNC BHI, and bioenergetics profiling in general, we applied the technique to MNCs from full-term pregnant and age-matched non-pregnant women. It is well documented that insulin sensitivity of adipose tissue and skeletal muscle of pregnant women changes from the second trimester to favour the passage of glucose across the placenta for use by the fetus [36]. The impact of this on haematopoietic cells and thereby immune function has not been considered, although there are numerous studies reporting differences in, for example, cytokine production with pregnancy [37–39]. Here we show that while there were no significant differences between any of the OP parameters, basal glycolysis and glycolytic capacity

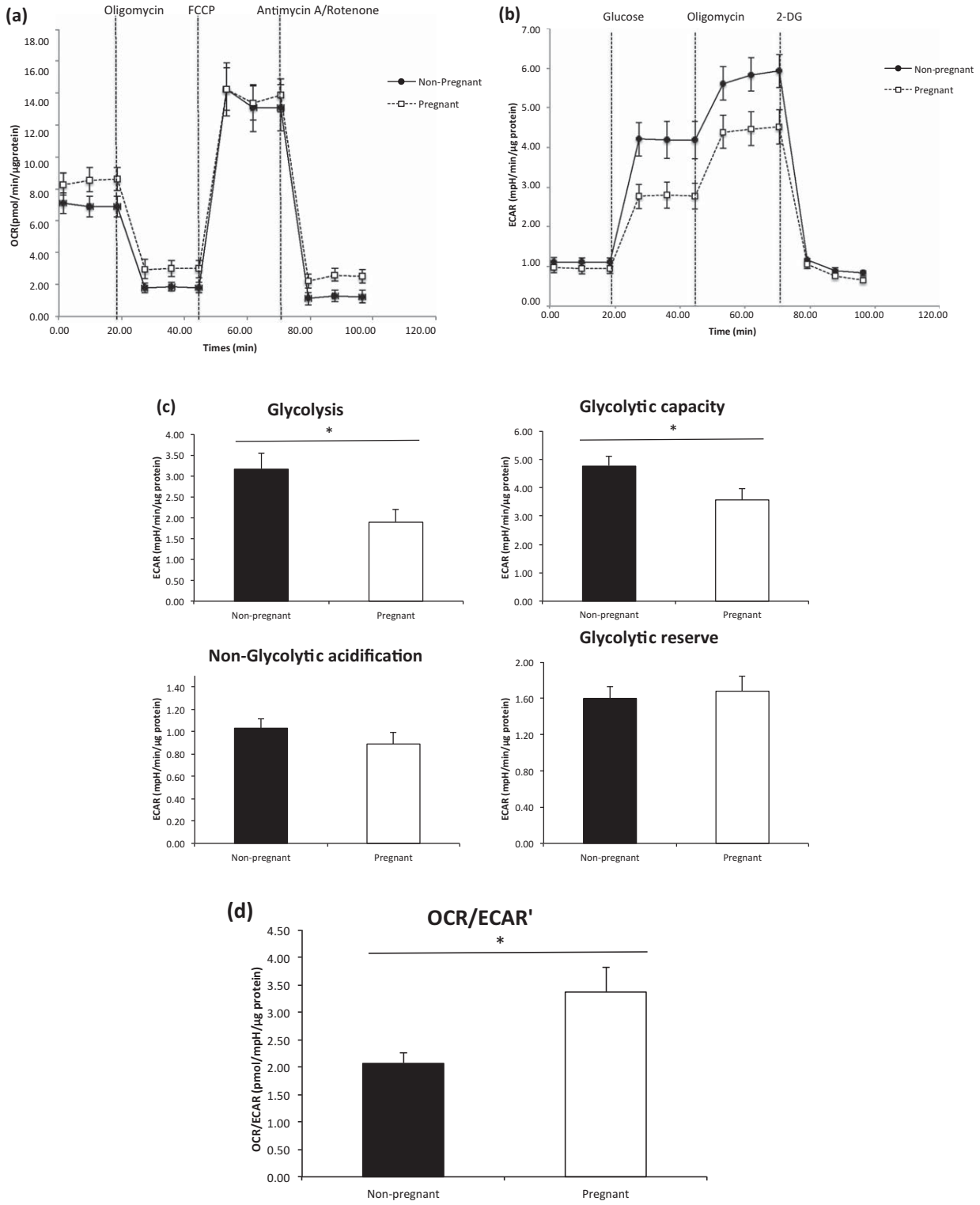

Fig. 5. Bioenergetic profile of mononuclear cells (MNCs) from non-pregnant *versus* pregnant women. MNCs from non-pregnant and pregnant donors were compared for (a) mitochondrial stress profile with injections oligomycin (0·75 µM), carbonyl cyanide-4-(trifluoromethoxy)phenylhydrazone (FCCP) (1 µM) and anti-mycin A/rotenone (both 1 µM); (b) glycolytic stress profile with injections of glucose (5·5 mM) and oligomycin (0·75 µM) and 2-DG (100 mM). (c) Comparative glycolytic respiratory parameters and (d) oxygen consumption rate/extracellular acidification (OCR/ECAR) ratio of MNCs from non-pregnant and pregnant women. All data are normalized to µg protein and shown as mean ± standard error of the mean ($n = 7$). Statistical differences are reported in the text, $^*P \leq 0{\cdot}05$.

Table 5. Comparative oxidative phosphorylation parameters of MNCs from non-pregnant *versus* pregnant women.

Respiratory parameter	Non-pregnant OCR (± s.e.m.; pmoles/min/μg protein)	Pregnant OCR (± s.e.m.; pmoles/min/μg protein)	*P*-value
Basal respiration	6·28 (± 0·54)	5·71 (± 0·52)	0·4639
ATP-linked respiration	3·29 (± 0·78)	3·88 (± 0·48)	0·5319
Non-mitochondrial respiration	2·44 (± 0·41)	1·23 (± 0·39)	0·0531
Maximal respiration	11·62 (± 1·28)	12·22 (± 1·36)	0·7559
Reserve respiratory capacity	5·34 (± 1·00)	6·50 (± 1·01)	0·4269
Proton leak	0·78 (± 0·19)	0·60 (± 0·18)	0·3759
BHI	15·66 (± 7·67)	30·22 (± 5·76)	0·1551

ATP = adenosine triphosphate; BHI = Bioenergetics Health Index; OCR = oxygen consumption rate; s.e.m. = standard error of the mean.

were reduced significantly in MNCs from pregnant women. Consequently, the OCR/ECAR ratio between the two groups differed significantly, and while the BHI increased with pregnancy this was not significant. MNCs from pregnant women are therefore more likely to utilize OP for their energy demands rather than glycolysis, as in non-pregnant women, and might fuel their energy needs through other substrates such as fatty acids that feed into OP [36]. These findings provide preliminary data showing that, like skeletal muscle and adipose tissue, blood MNCs in pregnancy down-regulate their use of glucose perhaps via decreased expression of pyruvate kinase [40], but this is now the focus of ongoing work.

The study of heterogeneous MNCs might lend itself to comparing the bioenergetics health index in clinical and translational settings, but does little to improve our understanding of how discrete leucocyte populations differ in their energy requirements in the resting and activated states. Further work with isolated individual leucocyte populations will provide further insight into the specific metabolic function of human immune cells. The bioenergetic profiles of isolated human monocytes, neutrophils and T cells have recently been identified revealing distinct differences between glycolysis and oxidative phosphorylation rates for each population postulated to reflect their biological roles [41].

While the study of mixed populations, as in this work, has its limitations, such an approach might provide a rapid turnaround of valuable bioenergetic information without the use of expensive single-population separation techniques, as demonstrated here by comparing MNCs from pregnant and non-pregnant women. MNCs from septic shock patients have reduced oxygen consumption and ATP synthesis [42], and extracellular flux analysis measured by high-resolution respiratory analyses could determine this quickly from small volumes of blood that would reflect the broad health status of the patient. This bioenergetic information has a potential role in identifying mitochondrial abnormalities, defining the revolutionary concept of the BHI [20]. The BHI could identify mitochondrial dysfunction that presents itself as increased non-mitochondrial respiration, increased proton leak and lower reserve capacity, suggesting that the mitochondria are damaged and unhealthy. Early identification could predict a patient's susceptibility to particular syndromes [20], and identification and monitoring of these stress parameters within metabolic disorders such as diabetes could facilitate precision medicine.

Acknowledgements

This work was supported by an Academic Expertise for Business (A4B) grant and a Life Sciences Research Network Wales Platform Grant. We thank the staff at the Joint Clinical Research Facility, and all blood donors who generously donated their blood towards this research.

Disclosure

The authors declare no conflicts of interest.

References

1 Pearce EL, Pearce EJ. Metabolic pathways in immune cell activation and quiescence. Immunity 2013; **38**:633–43.
2 Roiniotis J, Dinh H, Masendycz P *et al.* Hypoxia prolongs monocyte/macrophage survival and enhanced glycolysis is associated with their maturation under aerobic conditions. J Immunol 2009; **182**:7974–81.
3 Vander Heiden MG, Cantley LC, Thompson CB. Understanding the Warburg effect: the metabolic requirements of cell proliferation. Science 2009; **324**:1029–33.
4 Turner N, Cooney GJ, Kraegen EW, Bruce CR. Fatty acid metabolism, energy expenditure and insulin resistance in muscle. J Endocrinol 2014; **220**:T61–79.
5 Palsson-McDermott EM, O'Neill LA. The Warburg effect then and now: from cancer to inflammatory diseases. BioEssays 2013; **35**:965–73.
6 Macintyre AN, Rathmell JC. Activated lymphocytes as a metabolic model for carcinogenesis. Cancer Metab 2013; **1**:5.
7 Suchorolski MT, Paulson TG, Sanchez CA, Hockenbery D, Reid BJ. Warburg and Crabtree effects in premalignant Barrett's esophagus cell lines with active mitochondria. PLOS ONE 2013; **8**:e56884.
8 Marsin AS, Bouzin C, Bertrand L, Hue L. The stimulation of glycolysis by hypoxia in activated monocytes is mediated by AMP-activated protein kinase and inducible 6-phosphofructo-2-kinase. J Biol Chem 2002; **277**:30778–83.

9 Wahl DR, Byersdorfer CA, Ferrara JL, Opipari AW Jr, Glick GD. Distinct metabolic programs in activated T cells: opportunities for selective immunomodulation. Immunol Rev 2012; **249**:104–15.

10 Yang E, Fan L, Jiang Y, Doucette C, Fillmore S. Antimicrobial activity of bacteriocin-producing lactic acid bacteria isolated from cheeses and yogurts. AMB Express 2012; **2**:48.

11 Fangradt M, Hahne M, Gaber T *et al.* Human monocytes and macrophages differ in their mechanisms of adaptation to hypoxia. Arthritis Res Ther 2012; **14**:R181.

12 Freemerman AJ, Johnson AR, Sacks GN *et al.* Metabolic reprogramming of macrophages: glucose transporter (GLUT1)-mediated glucose metabolism drives a pro-inflammatory phenotype. J Biol Chem 2014; **289**:7884–96.

13 Doughty CA, Bleiman BF, Wagner DJ *et al.* Antigen receptor-mediated changes in glucose metabolism in B lymphocytes: role of phosphatidylinositol 3-kinase signaling in the glycolytic control of growth. Blood 2006; **107**:4458–65.

14 Kramer PA, Ravi S, Chacko B, Johnson MS, Darley-Usmar VM. A review of the mitochondrial and glycolytic metabolism in human platelets and leukocytes: implications for their use as bioenergetic biomarkers. Redox Biol 2014; **2**:206–10.

15 Cao MD, Sitter B, Bathen TF *et al.* Predicting long-term survival and treatment response in breast cancer patients receiving neoadjuvant chemotherapy by MR metabolic profiling. NMR Biomed 2012; **25**:369–78.

16 Keppel MP, Saucier N, Mah AY, Vogel TP, Cooper MA. Activation-specific metabolic requirements for NK cell IFN-gamma production. J Immunol 2015; **194**:1954–62.

17 Lund FE. Cytokine-producing B lymphocytes – key regulators of immunity. Curr Opin Immunol 2008; **20**:332–8.

18 Dietl K, Renner K, Dettmer K *et al.* Lactic acid and acidification inhibit TNF secretion and glycolysis of human monocytes. J Immunol 2010; **184**:1200–9.

19 Yabu M, Shime H, Hara H *et al.* IL-23-dependent and -independent enhancement pathways of IL-17A production by lactic acid. Int Immunol 2011; **23**:29–41.

20 Chacko BK, Kramer PA, Ravi S *et al.* The Bioenergetic Health Index: a new concept in mitochondrial translational research. Clin Sci 2014; **127**:367–73.

21 Sternfeld T, Tischleder A, Schuster M, Bogner JR. Mitochondrial membrane potential and apoptosis of blood mononuclear cells in untreated HIV-1 infected patients. HIV Med 2009; **10**:512–9.

22 Shikuma CM, Gerschenson M, Chow D *et al.* Mitochondrial oxidative phosphorylation protein levels in peripheral blood mononuclear cells correlate with levels in subcutaneous adipose tissue within samples differing by HIV and lipoatrophy status. AIDS Res Hum Retroviruses 2008; **24**:1255–62.

23 Ravi S, Mitchell T, Kramer PA, Chacko B, Darley-Usmar VM. Mitochondria in monocytes and macrophages – implications for translational and basic research. Int J Biochem Cell Biol 2014; **53**:202–7.

24 Pandzic Jaksic V, Gizdic B, Miletic Z, Ostovic KT, Jaksic O. Monocytes in metabolic disorders – opportunities for flow cytometry contributions. Coll Antropol 2010; **34**:319–25.

25 Keane KN, Calton EK, Cruzat VF, Soares MJ, Newsholme P. The impact of cryopreservation on human peripheral blood leukocyte bioenergetics. Clin Sci 2015; **128**:723–33.

26 Friedman JE, Kirwan JP, Jing M, Presley L, Catalano PM. Increased skeletal muscle tumor necrosis factor-alpha and impaired insulin signaling persist in obese women with gestational diabetes mellitus 1 year postpartum. Diabetes 2008; **57**:606–13.

27 Ong KK, Diderholm B, Salzano G *et al.* Pregnancy insulin, glucose, and BMI contribute to birth outcomes in nondiabetic mothers. Diabetes Care 2008; **31**:2193–7.

28 Hill BG, Benavides GA, Lancaster JR Jr *et al.* Integration of cellular bioenergetics with mitochondrial quality control and autophagy. Biol Chem 2012; **393**:1485–512.

29 Wu M, Neilson A, Swift AL *et al.* Multiparameter metabolic analysis reveals a close link between attenuated mitochondrial bioenergetic function and enhanced glycolysis dependency in human tumor cells. Am J Physiol Cell Physiol 2007; **292**:C125–36.

30 Kolodziejek AM, Caplan AB, Bohach GA, Paszczynski AJ, Minnich SA, Hovde CJ. Physiological levels of glucose induce membrane vesicle secretion and affect the lipid and protein composition of *Yersinia pestis* cell surfaces. Appl Environ Microbiol 2013; **79**:4509–14.

31 Lin Y, Berg AH, Iyengar P *et al.* The hyperglycemia-induced inflammatory response in adipocytes: the role of reactive oxygen species. J Biol Chem 2005; **280**:4617–26.

32 Wang SY, Hsu ML, Tzeng CH, Hsu HC, Ho CK. The influence of cryopreservation on cytokine production by human T lymphocytes. Cryobiology 1998; **37**:22–9.

33 Kreher CR, Dittrich MT, Guerkov R, Boehm BO, Tary-Lehmann M. CD4+ and CD8+ cells in cryopreserved human PBMC maintain full functionality in cytokine ELISPOT assays. J Immunol Methods 2003; **278**:79–93.

34 Larsen S, Wright-Paradis C, Gnaiger E, Helge JW, Boushel R. Cryopreservation of human skeletal muscle impairs mitochondrial function. Cryo Lett 2012; **33**:170–6.

35 O'Connell M, McClure N, Lewis SE. The effects of cryopreservation on sperm morphology, motility and mitochondrial function. Hum Reprod 2002; **17**:704–9.

36 Herrera E. Lipid metabolism in pregnancy and its consequences in the fetus and newborn. Endocrine 2002; **19**:43–55.

37 Vanders RL, Gibson PG, Wark PA, Murphy VE. Alterations in inflammatory, antiviral and regulatory cytokine responses in peripheral blood mononuclear cells from pregnant women with asthma. Respirology 2013; **18**:827–33.

38 Breckler LA, Hale J, Taylor A, Dunstan JA, Thornton CA, Prescott SL. Pregnancy IFN-gamma responses to foetal alloantigens are altered by maternal allergy and gravidity status. Allergy 2008; **63**:1473–80.

39 Sakai M, Tsuda H, Tanebe K, Sasaki Y, Saito S. Interleukin-12 secretion by peripheral blood mononuclear cells is decreased in normal pregnant subjects and increased in preeclamptic patients. Am J Reprod Immunol 2002; **47**:91–7.

40 Xu Y, Madsen-Bouterse SA, Romero R *et al.* Leukocyte pyruvate kinase expression is reduced in normal human pregnancy but not in pre-eclampsia. Am J Reprod Immunol 2010; **64**:137–51.

41 Chacko BK, Kramer PA, Ravi S *et al.* Methods for defining distinct bioenergetic profiles in platelets, lymphocytes, monocytes, and neutrophils, and the oxidative burst from human blood. Lab Invest 2013; **93**:690–700.

42 Japiassu AM, Santiago AP, d'Avila JC *et al.* Bioenergetic failure of human peripheral blood monocytes in patients with septic shock is mediated by reduced F1Fo adenosine-5'-triphosphate synthase activity. Crit Care Med 2011; **39**:1056–63.